Hybridizing FD-TD Analysis with Unconditionally Stable FEM for Objects of Curved Boundary

Ruey-Beei Wu† and Tatsuo Itoh‡

†Department of Electrical Engineering
National Taiwan University, Taipei, Taiwan, ROC

‡ Electrical Engineering Department
University of California, Los Angeles, USA

Abstract

A novel unconditionally stable finite element scheme is incorporated to the conventional FD-TD analysis for solving the Maxwell's equations associated with objects with curved boundary. It is applied to electromagnetic scattering of two dimensional arbitrarily shaped dielectric cylinders to demonstrate its advantages in accuracy, stability, computational efficiency, and programming ease.

Introduction

The FD-TD analysis has been prevalently applied to deal with various electromagnetic problems. Its original form works excellently for structures which can fit well into Cartesian coordinates [1]. However, it suffers from the disadvantage that an accurate staircase approximation to a structure with curved boundary usually requires a very fine mesh and, consequently, a very small time step in time marching due to the stability constraint. Exploiting conformity is one way to alleviate the staircasing approximation. Several researchers have proposed the conformal schemes and employed them to the solution region either globally [2,3] or locally [4,5,6].

To better model the arbitrary boundary, the more flexible finite element method (FEM) has been investigated recently [7,8]. In addition to a sophisticated management and vast memory storage for the bookkeeping system in FEM, it requires in each time step the solution of a large system of simultaneous equations, which is quite time consuming even employing the sparse matrix technique. This makes it especially desirable to confine the FEM solution region as close to the curved boundary as possible. Also, the division in FEM may sometimes unavoidably involve a very fine mesh locally, which causes a serious stability concern. A small time step to ensure the algorithm stable in the region with fine mesh may in turn substantially deteriorate the overall computational efficiency.

This paper proposes a hybrid method which employs the conventional FD-TD in most of the regular region and the FEM in the junction region near the curved boundary. This strategy preserves all the FD-TD advantages in most of the regular region while resorts to FEM just enough to model the curved boundary. Also incorporated is a scheme with unconditional stability which circumvents the stability problem without any additional computational load during the time marching. As a result, the mesh division in FEM can be made arbitrarily fine to fit the curved boundary while the stability is constrained only by the conventional FD-TD in the regular region.

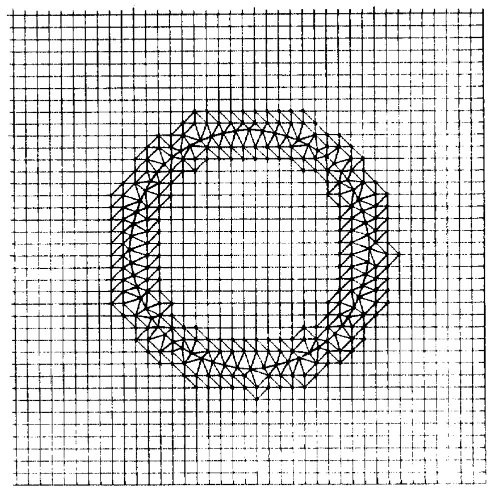

Fig. 1. Division of solution region.

Time Marching Scheme

Consider a dielectric object of a curved boundary shown in Fig.1. The solution region is divided into the regular and junction regions. The rectangular mesh in FD-TD algorithm is employed in the regular region which spans both the exterior free space and the interior

WE 3F

CH3577-4/95/0000-0833$01.00 © 1995 IEEE

dielectric medium a certain distance from the curved boundary. Depending on the division size Δ in rectangular FD-TD, the junction region usually spans three to five division units and encloses the curved boundary to both sides. Due to the flexibility offered by FEM, it is not difficult to set up a mesh in the junction region which conforms the curved boundary to the rectangular FD-TD mesh. It is worthy noticing in Fig.1 that not only the boundary (called exterior boundary) of the junction region but also the mesh points on the boundary (called secondary boundary) next to the exterior boundary fits the FD-TD mesh exactly.

The time domain analysis for solving Maxwell's equations can be described by the time marching scheme. Following the conventions in the FD-TD algorithm, the discretizations are interleaved in both time and space. Let $H_{FD}^{n-\frac{1}{2}}$ and E_{FD}^{n} be the magnetic and electric fields in the regular region at time instants $n-\frac{1}{2}$ and n, respectively. In the junction region, E_{FEM}^{n} denotes the electric field at the time instant n, among which $E_{FEM,B}^{n}$ and $E_{FEM,I}^{n}$ are the fields on the exterior and secondary boundaries, respectively. It deserves mentioning that $E_{FEM,B}^{n}$ and $E_{FEM,I}^{n}$ coincide with the FD-TD mesh. Actually, the secondary boundary of the junction region serves as the exterior boundary of the regular region, and vice versa.

Given the electric fields E_{FD}^{n}, $E_{FEM,B}^{n}$, and $E_{FEM,I}^{n}$, one can update the magnetic field by applying the Faraday's law [1]. Not only $H_{FD}^{n+1/2}$, the field in the regular region but also $H_{FEM,IB}^{n+1/2}$, the field on the center surface between exterior and secondary boundaries become available. Based on them, one can proceed to update the electric field by applying the Ampere's law [1]. Here, both E_{FD}^{n+1} and $E_{FEM,B}^{n+1}$ can be determined.

It is next desired to solve the electric field in the junction region at the time instant $n+1$. This is an initial value problem in time with E_{FEM}^{n} being the initial condition as well as a boundary value problem in space with $E_{FEM,B}^{n+1}$ being the boundary condition.

Unconditionally Stable FEM Scheme

The unconditionally stable FEM (US-FEM) scheme to be employed here follows the basic idea of Crank-Nicolson formulation for hyperbolic partial differential equations. It can be applied no matter that the differential operator in space is modeled by finite difference or finite element based on node or edge representation. For simplicity sake, the edge representation recently proposed in [8] is employed here.

By a fruitful choice of the edge basis, the fields can be updated by [8]

$$\frac{\delta H_i}{\Delta_t} = \frac{1}{\mu A_i}\sum_j E_j \ell_j \quad ; \quad \sum_i c_i \frac{\delta E_i}{\Delta_t} = \sum_j d_j H_j \quad (1)$$

where the central difference operator δ is defined by $\delta F \equiv F^{n+\frac{1}{2}} - F^{n-\frac{1}{2}}$, A_i is the area of the i^{th} face, E_j and ℓ_j are the surrounding E's and line segments, and c_i's and d_j's are some coefficients.

In the conventional time domain analysis, the time derivative is modeled by forward central difference while the fields in the right hand sides of (1) are the values at the central time instant. The US-FEM scheme introduces an additional average operator in time

$$\theta F \equiv \frac{F^{n+\frac{1}{2}} + F^{n-\frac{1}{2}}}{2} \quad (2)$$

to the right hand sides. Combining the resultant two equations in (1) yields a system of equations which can be written in the matrix form

$$[C]\delta^2\overline{E} = -[D]\theta^2\overline{E} \quad (3)$$

where $\overline{E}$ denotes the vector of the desired electric fields in the junction region.

By the definition of the operators δ and θ, the final governing equation for the electric field at time instant $n+1$ can be written as

$$\begin{aligned}([C] + \frac{1}{4}[D])\overline{E}^{n+1} &= \\ 2([C] - \frac{1}{4}[D])\overline{E}^{n} &- ([C] + \frac{1}{4}[D])\overline{E}^{n-1} \quad (4)\end{aligned}$$

Given the boundary field $E_{FEM,S}^{n+1}$, all the fields in the junction region E_{FEM}^{n+1} can be solved from (4). Although with more complicated expression, the matrices in (4) have the same sparsity as the original ones in (1). After suitable decomposition, both take same computation time in the solution of the desired interior field at each time step.

It is not difficult to show that (4) is unconditionally stable. The matrix $[C]$ denotes equivalent area and is obviously positive definite. The matrix $[D]$ corresponds to the modeling of the Laplacian operator, $-\nabla^2$, in space by FEM. Its positive definiteness can also be ensured since the Laplacian operator subject to Dirichlet boundary condition is positive definite. As a result, (4) can be shown to be always stable since all the eigenvalues of the matrix $([C] + \frac{1}{4}[D])^{-1}([C] - \frac{1}{4}[D])$ have magnitudes smaller than unity.

Stability, Accuracy, and Computational Efficiency

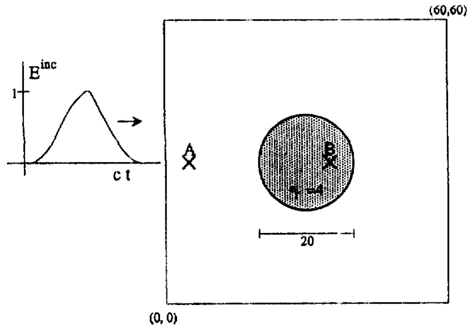

Fig. 2. Example problem of a dielectric circular cylinder illuminated by an incident Gaussian TM wave.

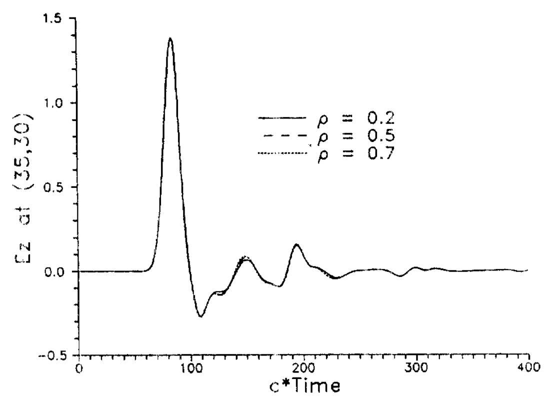

Fig 3. Calculated total field inside the dielectric cylinder with $\Delta = 1cm$ and time step ratio ρ as a parameter.

To investigate its numerical aspects, the present formulation is applied to the electromagnetic scattering of arbitrarily shaped two-dimensional dielectric objects. Fig.2 shows the example problem considered in this paper. A circular cylinder of dielectric constant $\epsilon_r = 4.0$ and radius of $10cm$ is normally illuminated by a Gaussian pulse of three-sigma pulse width $20cm$. The transient response up to $c \cdot t = 400cm$ are of interest.

Fig.3 shows the total field at an interior point B with $\Delta = 1cm$ and time step ratio $\rho = \frac{c\Delta_t}{\Delta}$ as a parameter. It is found that the present method remains stable even if $\rho = 0.7$. Actually, it is the conventional FD-TD algorithm rather than the present US-FEM scheme which imposes the stability constraint ($\rho \leq \sqrt{2}$).

Fig.4(a) investigates the convergency of the present

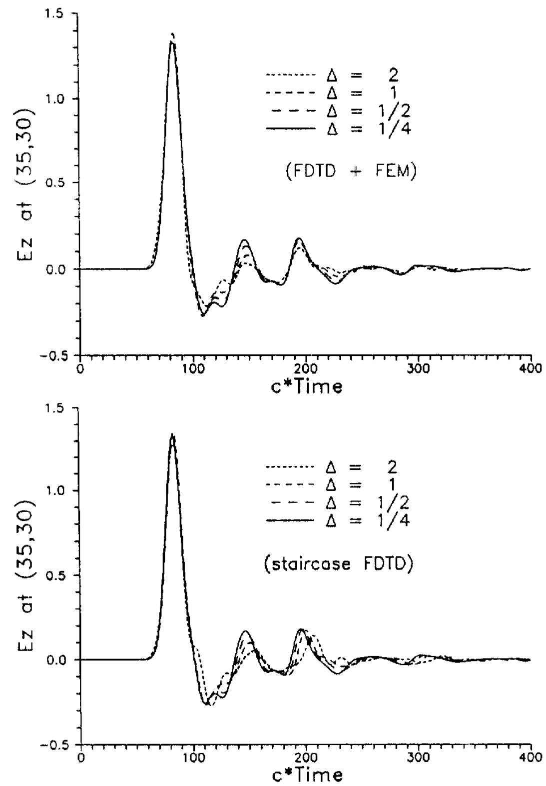

Fig. 4. Calculated total field inside the dielectric cylinder with $\rho = 0.5$ and Δ as a parameter. Comparison between (a) hybrid method and (b) conventional FD-TD algorithm with staircase approximation.

hybrid method with $\rho = 0.5$ and Δ as a parameter. It is interesting to notice the focusing effects due to the circular dielectric cylinder. For comparison sake, the results by the conventional FD-TD algorithm with a simple staircase approximation are presented in Fig.4(b). Although both methods with a very fine division ($\Delta = \frac{1}{4}cm$) yield almost identical results, the staircase FD-TD results suffer relatively larger discrepancy in the transient response.

Fig.5(a) and (b) compare the scattered fields calculated by these two methods at an exterior point A. When the division is rough, the results of either method show some discrepancy. It is hard to say which one is better at a particular time instant. However, the figures clearly show that the results obtained by the present hybrid method converge more steadily and depict the arrival time of each late time ripple more accurately.

Finally to be addressed is the computational effi-

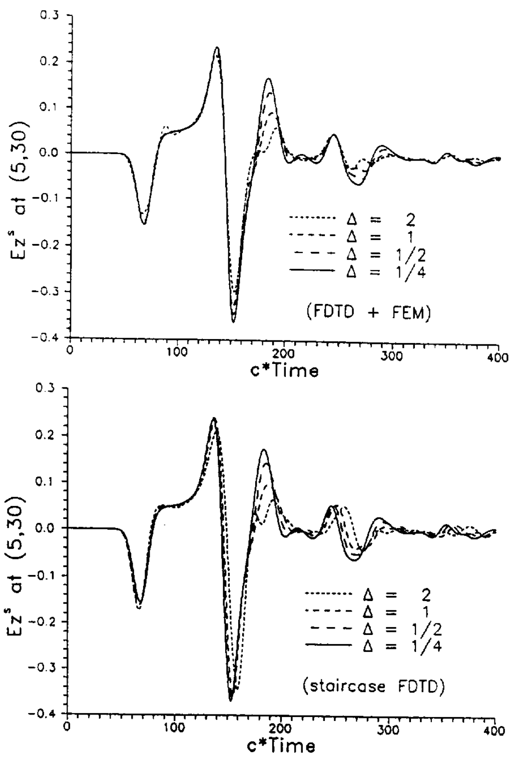

Fig. 5. Calculated scattered field in free space region with $\rho = 0.5$ and Δ as a parameter. Comparison between (a) hybrid method and (b) conventional FD-TD algorithm with staircase approximation.

ciency of the present hybrid method. Due to the incorporation of FEM, the method requires additional computation time and memory in mesh generation, matrix calculation, and matrix decomposition during the preprocessing as well as in matrix solution during the time marching. Table I compares the required CPU time and memory storage to those in conventional FD-TD algorithm. Let $N = \frac{60}{\Delta}$ be the number of divisions in each dimension. The total required memory and execution time per step for FD-TD analysis are proportional to N^2. On the other hand, the additional memory storage and time for FEM analysis increase roughly proportionally to N. As a result, the overhad of the present hybrid method becomes relatively smaller for a finer mesh. For the case with a 300×300 mesh, the overhead is found to be only 10% in computation time and 13% in memory requirement.

References

[1] K. S. Yee, "Numerical solution of initial boundary value problems in isotropic media," *IEEE Trans. Antennas Propagat.*, vol. AP-14, pp. 302-307, May 1966.

[2] R. Holland, "Finite-difference solutions of Maxwell's equations in generalized non-orthogonal coordinates," *IEEE Trans. Nucl. Sci.*, vol. NS-30, pp. 4589-4591, 1983.

[3] J. F. Lee, R. Palandech, and R. Mittra, "Modeling three-dimensional discontinuities in waveguides using nonorthogonal FDTD algorithm," *IEEE Trans. Microwave Theory Tech.*, vol. MTT-40, pp. 346-352, Feb. 1992.

[4] K. S. Yee, J. S. Chen, and A. H. Chang, "Conformal finite-difference time-domain (FD-TD) with overlapping grid," *IEEE Trans. Antennas Propagat.*, vol. AP-40, pp. 1068-1075, Sept. 1992.

[5] T. G. Jurgens, A. Talflove, K. Umashanker, and T. G. Moore, "Finite-difference time-domain modeling of curved surfaces," *IEEE Trans. Antennas Propagat.*, vol. AP-40, pp. 357-366, April 1992.

[6] J. Fang and J. Ren, "A locally conformed finite-difference time-domain algorithm of modeling arbitrary shape planar metal strips," *IEEE Trans. Microwave Theory Tech.*, vol. MTT-41, pp. 830-838, May 1993.

[7] J. F. Lee, "WETD-a finite element time-domain approach for solving Maxwell's equations," *IEEE Microwave Guided Wave Lett.*, vol. 4, pp. 11-13, Jan. 1994.

[8] C. H. Thng and R. C. Booton, "Edge-element time-domain method for solving Maxwell's equations," *IEEE MTT-S Digest*, pp. 693-696, May 1994.

TABLE I

Comparison of CPU time and memory requirement between hybrid method and conventional FD-TD ($\rho = 0.5$)

Δ	mesh $N \times N$	method	pre-processing time	pre-processing memory	time marching time/steps	time marching memory	FEM overhead time	FEM overhead memory
2.0	30×30	hybrid	2.25	9,840	4.56/ 400	6,228	153%	257%
		FD-TD	–	–	2.69/ 400	2,760		
1.0	60×60	hybrid	2.69	19,680	24.83/ 800	18,146	61%	80%
		FD-TD	–	–	17.13/ 800	10,920		
0.5	120×120	hybrid	4.29	39,360	167.44/1600	57,622	30%	33%
		FD-TD	–	–	132.32/1600	43,440		
0.25	240×240	hybrid	9.89	97,920	1106.26/3200	201,630	13%	16%
		FD-TD	–	–	984.40/3200	173,280		
0.2	300×300	hybrid	13.57	139,633	2217.68/4000	304,191	10%	13%
		FD-TD	–	–	2019.92/4000	268,801		

Program is executed in a notebook PC (TwinHead SlimNote DX2-66MHz).

The units of time and memory are *sec* and 4 bytes, respectively.